

Discussion

Kellogg, P. J.: All the orbits which you showed turned around nearer to the equator than the Alfvén perturbation theory would predict, that is, they were better trapped. Surely there must also be orbits which turn farther from the equator, and I wonder if there is a reason why none of these were found.

Gall, R.: Only orbits corresponding to particles of higher energy ($\gamma < 2$) reflect below the adiabatic reflection latitude. The reason why these orbits reflect below the adiabatic mirror point is the following: these orbits are nearly asymptotic to periodic orbits, and many of the periodic orbits never reach the adiabatic mirror points.

I would like to stress that the adiabatic conditions guides us as far as the mirror altitude is concerned. Trapping however occurs also for energies for which $\mu \neq \text{cst.}$, as long as $\gamma > 1$.

JOURNAL OF THE PHYSICAL SOCIETY OF JAPAN Vol. 17, SUPPLEMENT A-II, 1962
INTERNATIONAL CONFERENCE ON COSMIC RAYS AND THE EARTH STORM Part II

II-2-8. Mechanism of the Mirror Point Loss

S. FUKUI, S. HAYAKAWA, H. NISHIMURA
and H. OBAYASHI

Physical Institute, Nagoya University, Nagoya, Japan

In cosmic ray physics various problems are concerned with the behavior of charged particles in a magnetic field, *i.e.*, formation and stability of the radiation belts, the observed anisotropy of the heavy primaries¹⁾, and so on.

We have made a simple model experiment²⁾ in order to get characteristic information about the loss mechanism of electrons from a magnetic bottle. There may be several causes to make a trapped electron escape, for example, (i) the scattering with the residual gas atoms³⁾, (ii) the energy loss due to ionization (iii) the break-down of the adiabatic invariance^{4) 5)}. The purpose of our experiment is to distinguish them from one another with varying conditions and to find the explanation of the cosmic ray phenomena. Here we give some of the preliminary results so far obtained.

As shown schematically in Fig. 1, a pair of air core coils are connected coaxially by a cylindrical brass vacuum chamber, an electron gun is set near the center of the chamber, and a collimated electron beam of 1.5

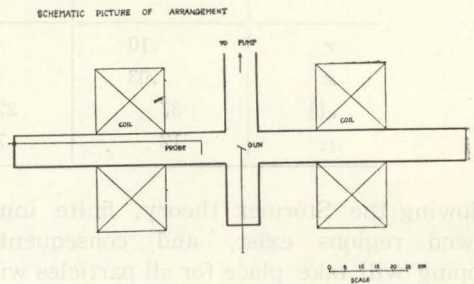


Fig. 1. Schematic picture of arrangement.

Kev is injected with a pitch angle $\alpha_0 = 30^\circ \pm 5^\circ$. It is very important to make the electron gun as small as possible for having definite injection conditions, for minimizing the shadow effect, and for avoiding the effect of the magnetic field in an accelerating section. The gun used is of $\sim 1 \text{ cm} \times 1 \text{ cm}$ ϕ and gives a current of the order of mA. Effects of space charge or plasma motion in the chamber are negligible. Though both of the stationary and pulsive injections are possible, most parts of observations have been done with the pulse of 5 μsec duration. Currents

have been detected by pintype probes which are fixed on a shaft and can be moved by translating or rotating the shaft. The probe currents were displayed on an oscilloscope.

Fig. 2 indicates the magnetic field strength along the axis. The maximum mirror ratio

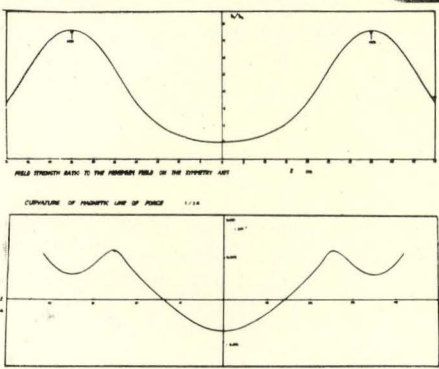


Fig. 2. Field strength ratio to the minimum field on the symmetry axis and curvature of magnetic line of force ($1/rR$).

is 7.6, which corresponds to the loss cone of about 21.2° of the initial pitch angle α_0 . The absolute field strength can be adjusted by controlling the exciting current of the coils. In the present studies the magnitude of the field is fixed so as to give a gyro-radius of 2 cm at the center for a 1.5 Kev electron.

The curvature ($1/R$) of a line of force divided by the radial distance r is also shown in Fig. 2. As $r \leq 5$ cm in the experimental region, the radius of curvature R is about 100 cm, namely much larger than the gyro-radius.

The characteristic features of the apparatus were shown in Tab. I. A vacuum of 10^{-6} mmHg is prepared and various pressures, up to 10^{-3} mmHg, of helium and argon are added. It should be noted that the Coulomb scatter-

Table I. Characteristic features of apparatus.

Magnetic field:	200-1500 gauss inside a coil 50- 500 gauss in the central part
Maximum mirror ratio:	7.6
Vacuum chamber:	10 cm ϕ \times 100 cm
Vacuum and gases filled:	Vacuum $\approx 10^{-6}$ mmHg He or Ar \approx up to 10^{-3} mmHg
Electron injected:	Energy=0.5-1.5 Kev Current ≤ 10 mA Collimation $\approx \pm 5^\circ$ Pulse duration=3-10 μ sec

ing and the atomic collision are dependent on the kind of gas, or Z and A , while the ionization energy loss of an electron is mainly governed by the pressure of gas. The possible evidence of the non-adiabaticity will be expected irrespective of gas conditions, if any.

Since the direction of the field vector is nearly parallel everywhere, the variable concerning the field can be expanded about the axis. The terms depending on the curved nature of lines of force can be considered as perturbation. The first order theory can be shown to coincide with the ordinary guiding center picture for gyrating electrons. Fig. 3 shows the calculated azimuthal drift angles of the guiding center as functions of its axial position.

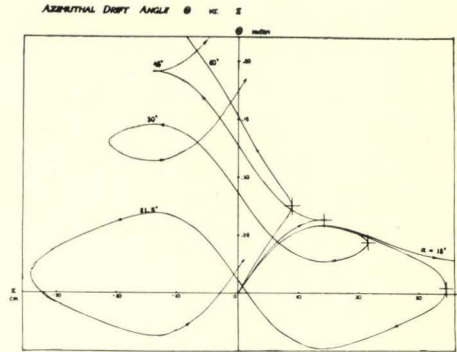


Fig. 3. Azimuthal drift angle vs axial distance.

In our device most of the trapped electrons are disturbed by the gun system, because of its relatively large size. It was estimated that some 90% of the electrons of the initial beam strike the gun system in the first 3 or 4 transit periods. After about 5 transit periods ($\geq 0.4 \mu$ sec) the azimuthal drift carries the beam away from the gun. Only $\sim 10\%$ of the electrons remain in the trapping region and are subject to the loss mechanisms we are investigating. Now it must be noted that electrons found at the place out of the maximum field should be the ones escaped from the trapping region in any way. The observed intensity of leak currents gives the energy and density distributions of electrons confined in the bottle.

Characteristic times for the trapped particles are estimated and tabulated in Tab. II. The scattering probability of slow electrons

Table II. Characteristic times for trapped particles.

gas.	Mean lifetime of scatterings for 1.5 kev electrons τ_f	Mean lifetime of scatterings for slow electrons (~ 1 ev) τ_s	Mean lifetime of ionization collisions for electrons τ_c
6×10^{-4} mmHg Ar	0.2 μ sec	7 μ sec	0.2 μ sec
4×10^{-4} mmHg He	4 μ sec	1.4 μ sec	0.1 μ sec

in argon shows strong dependence on the electron energy, while in helium it is not sensitive. The injected fast electrons produce the slow electrons and ions through ionization along the path of the beam. The energy loss of the fast electron is 30 eV in a single collision, and so the energy loss will be a minor cause of its escape. Lifetime τ_c in Tab. II is, therefore, considered as the production lifetime for slow electrons and ions. These slow electrons and ions produced are also trapped or scattered. Fast and slow electrons and ions can be distinguished by the probe of various bias potentials, say, +90, 0, -90V.

In the present case the trapped fast (1.5 KeV) electrons will be lost mainly by scattering process, whose characteristic time is τ_f . In order to pass the bottle neck, electrons should be suffered from several collisions, because the necessary change in the pitch angle is as large as $\geq 40^\circ$. The oscilloscope figures can be expected to have the decay slope characterized by several times of τ_f .

In Figs. 4~7 typical oscilloscope displays are shown. For example, in Fig. 7 the first peak is contributed by fast electrons scattered from the gun system, and the decay slope is regarded as by scatterings and will give an experimental estimated of τ_f . The second peak is composed of slow electrons and its position is related to τ_c and the decay slope gives τ_s . Comparing the experimental values with the calculated ones given in Tab. II, the latter should be multiplied by some factors because the calculation is for single process whereas an actual escape will take place after several collisions as mentioned above. There is no serious inconsistency between observation and calculation.

Finally we make a remark on the adiabatic

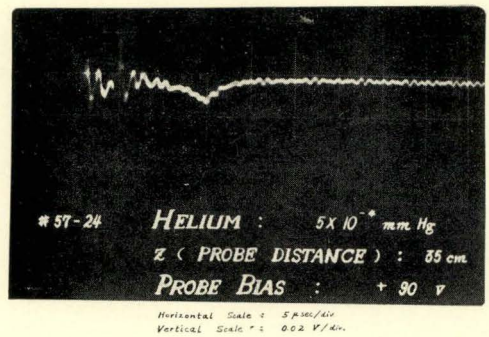


Fig. 4. Oscilloscope display of observed current. He (+90V).

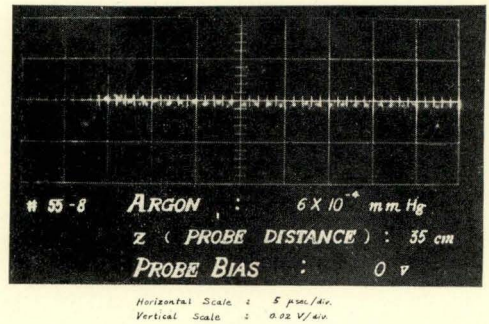


Fig. 5. Oscilloscope display of observed current. Ar (0V).

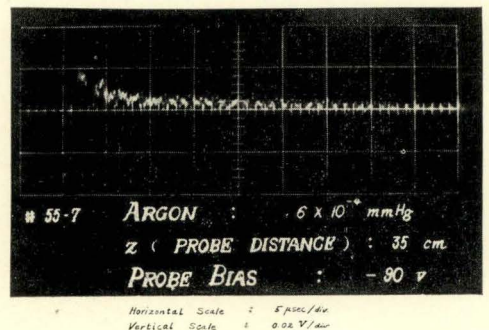


Fig. 6. Oscilloscope display of observed current. Ar (-90V).

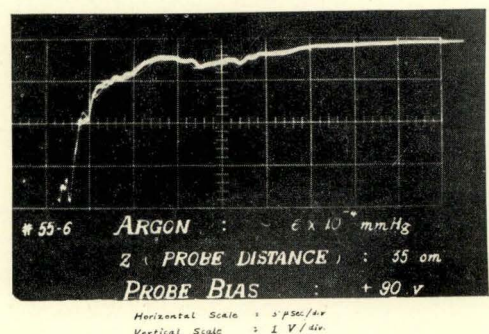


Fig. 7. Oscilloscope display of observed current. Ar (+90V).

invariance of the magnetic moment of a gyrating particle. In theoretical treatments⁶⁾ the whole motion of an electron is decomposed into three parts within the canonical formalism, *i.e.*, the gyration, the longitudinal drift, and the azimuthal drift. In a homogeneous field, namely the zeroth order theory, they can be separated. The magnetic moment is introduced as the action integral of the gyration mode: $J^{(0)} = \oint P^{(0)} dQ^{(0)}$. Taking into account the perturbation, the action integral will change the form and the old $J^{(0)}$ is no more a constant but will oscillate around

a new $J^{(1)} = \oint P^{(1)} dQ^{(1)}$. Variations of J were calculated for our system and shown in Fig. 8. In the present case, however, the net variation of J is 0.2% or less of its initial value and cannot be expected to reveal its effect within the present accuracy of the experiment. But this kind of non-adiabaticity might cause a part of the proton instability in the outer radiation belt.

References

- 1) S. Fukui, S. Hayakawa, H. Nishimura and H. Obayashi: paper presented at this conference, III-3-5.
- 2) A similar experiment to ours is published. G. M. Antropov, V. A. Beljaev and M. K. Romanovskij: Plasma Physics and Problems of Controlled Thermonuclear Reactions, III (1958) 250.
- 3) J. A. Welch Jr. and W. A. Whitaker: J. Geophys. Res. **64** (1959) 909.
- 4) A. Garren *et al.*: 2nd United Nations Int. Conf. Peaceful Uses Atomic Energy (1958, Geneva) **31** 65, p. 383.
- 5) P. O. Vandervoort: Ann. of Phys. **12** (1961) 436.
- 6) H. Obayashi: Prog. Theor. Phys. **25** (1961) 297.

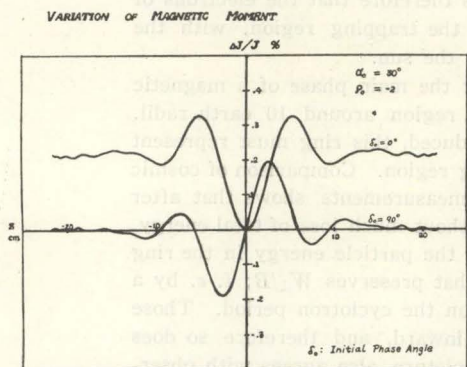


Fig. 8. Variation of magnetic moment.

Discussion

Kellogg, P. J.: The results which have just been presented bear very importantly on the mechanism of breakdown of adiabatic invariance proposed by Singer to account for the outer edge of the Van Allen proton belt. But most of the results can be understood in terms of the next term in the adiabatic invariant w_{\perp}/B , (which is only the first term in the power series for the true adiabatic invariant) and represent oscillations of w_{\perp}/B but not secular drifts. Is there more information on the secular drifts (which I confess I do not understand)?

Hayakawa, S.: I hope I could make this point a little bit clearer. Our theory is based on the Hamiltonian formalism which can separate three modes of motion unambiguously. Accordingly, we are able to show the coupling between the gyration mode and the longitudinal oscillation mode; the energy of motion is exchanged between these two modes like in the double pendulum. At some moments, therefore, the longitudinal energy becomes so large that particles can go over the position of the maximum field strength, if it has a lucky (or unlucky) phase.